Human Pathology (2019) **91**, 43–51

ELSEVIER

Human PATHOLOGY

www.elsevier.com/locate/humpath

Original contribution

Vascular density of histologically benign breast tissue from women with breast cancer: associations with tissue composition and tumor characteristics☆,☆☆

Ashley M. Fuller PhD[a,1], Linnea T. Olsson BS, BA[b], Bentley R. Midkiff BS[c], Erin L. Kirk MS[b], Kirk K. McNaughton BS[d], Benjamin C. Calhoun MD, PhD[a,c], Melissa A. Troester PhD, MPH[a,b,c,*]

[a]*Department of Pathology and Laboratory Medicine, The University of North Carolina School of Medicine, Chapel Hill, NC, 27599, USA*
[b]*Department of Epidemiology, Gillings School of Global Public Health, The University of North Carolina, Chapel Hill, NC, 27599, USA*
[c]*Lineberger Comprehensive Cancer Center, The University of North Carolina, Chapel Hill, NC, 27599, USA*
[d]*Department of Cell Biology and Physiology, The University of North Carolina School of Medicine, Chapel Hill, NC, 27599, USA*

Received 20 February 2019; revised 17 June 2019; accepted 19 June 2019

Keywords:
CD31;
Digital histology;
Microenvironment;
Normal breast;
Vasculature

Summary In breast tumors, it is well established that intratumoral angiogenesis is crucial for malignant progression, but little is known about the vascular characteristics of extratumoral, cancer-adjacent breast. Genome-wide transcriptional data suggest that extratumoral microenvironments may influence breast cancer phenotypes; thus, histologic features of cancer-adjacent tissue may also have clinical implications. To this end, we developed a digital algorithm to quantitate vascular density in approximately 300 histologically benign tissue specimens from breast cancer patients enrolled in the UNC Normal Breast Study (NBS). Specimens were stained for CD31, and vascular content was compared to demographic variables, tissue composition metrics, and tumor molecular features. We observed that the vascular density of cancer-adjacent breast was significantly higher in older and obese women, and was strongly associated with breast adipose tissue content. Consistent with observations that older and heavier women experience higher frequencies of ER_+ disease, higher extratumoral vessel density was also significantly associated with positive prognostic tumor features such as lower stage, negative nodal status, and smaller size (<2 cm). These results reveal biological relationships between extratumoral vascular content and body size, breast tissue

☆ Competing interests: All authors declare that there are no conflicts of interest to report.

☆☆ Funding/Support: This work was supported by P30 ES010126, U01 CA179715, P50 CA058223, U01 ES19472, and the Komen Foundation Graduate Training in Disparities Research program. AMF also received support from the UNC Integrated Vascular Biology program (T32 HL069768) and the UNC Royster Society of Fellows. The UNC Translational Pathology Laboratory is supported in part by grants from the NCI (P30 CA016086-42), NIH (U54 CA156733), NIEHS (P30 ES010126-17), North Carolina Biotechnology Center (2015-IDG-1007), and University Cancer Research Fund.

* Corresponding author at: 253 Rosenau Hall, CB #7435, Chapel Hill, NC, 27599.
E-mail addresses: ashley.fuller@pennmedicine.upenn.edu (A. M. Fuller), lolsson@live.unc.edu (L. T. Olsson), midkiff1@email.unc.edu (B. R. Midkiff), ekirk@email.unc.edu (E. L. Kirk), macone@med.unc.edu (K. K. McNaughton), ben.calhoun@unchealth.unc.edu (B. C. Calhoun), troester@unc.edu (M. A. Troester).
[1] Present address: Department of Pathology and Laboratory Medicine and Abramson Family Cancer Research Institute, The University of Pennsylvania Perelman School of Medicine, Philadelphia, PA, 19104, USA.

https://doi.org/10.1016/j.humpath.2019.06.003
0046-8177/© 2019 Published by Elsevier Inc.

composition, and tumor characteristics, and suggest biological plausibility for the relationship between weight gain (and corresponding breast tissue changes) and breast cancer progression.
© 2019 Published by Elsevier Inc.

1. Introduction

Solid tumors, including breast cancers, must initiate angiogenesis to grow beyond a size of 1–2 mm^3 [1]. While intratumoral vasculature has been relatively well-studied (reviewed by Siemann [2]), very little research has addressed the vascular characteristics of extratumoral microenvironments, nor those of the histologically benign tissue adjacent to breast cancers. A growing body of evidence indicates that extratumoral microenvironments may play a role in breast cancer progression. For example, the gene expression signatures of tumor-adjacent breast resemble those of the associated cancer [3,4], and can predict outcomes in some patient groups such as ER^+ cases [5-7]. Correlates of tissue composition, such as obesity, have also been shown to predict breast cancer patient outcomes, with inverse associations between body mass index (BMI) and survival having been reported across breast cancer subtypes, and particularly in the context of ER^+ disease [8-10]. However, histologic studies of extratumoral and benign breast microenvironments, particularly with regard to vascular characteristics, have only been conducted using tissue specimens from a small or unspecified number of demographically homogenous women [11,12], highlighting the importance of further study in this area.

In this study of approximately 300 specimens from 228 women, we employed a digital histologic approach to quantitate vascular density (number of vessels/mm^2 of tissue) in histologically benign breast tissue from women with breast cancer. We hypothesized that cancer-adjacent breast vessel density may be associated with tumor features, either through relationships with patient characteristics, or because vasculature supports tumor growth or enables selection of more adaptive phenotypes.

2. Materials and methods

2.1. Study population

Biospecimens from the University of North Carolina Normal Breast Study (UNC NBS) [13,14] were used following a protocol approved by the University of North Carolina School of Medicine Institutional Review Board. Briefly, the UNC NBS is a hospital-based study of normal breast tissue and breast cancer microenvironments. Women undergoing breast surgeries (excisional biopsy, lumpectomy, mastectomy, reduction mammoplasty, or other cosmetic procedure) at UNC Hospitals between October 2009 and April 2013 were eligible to participate if they were at least 18 years of age, English-speaking, and consented to donate tissue during their surgery. As previously described [13,14], all participants donated grossly normal-appearing tissue as assessed by pathology assistants at UNC; the distance of each cancer-adjacent specimen from the corresponding primary tumor was categorized as <1 cm, 1–4 cm, or >4 cm. Tissue was snap-frozen in liquid nitrogen. Patients also provided demographic, lifestyle, and breast cancer risk factor exposure data through a telephone interview, and medical records abstraction was performed to obtain anthropometric and medical history data. Medical records follow-up is continuing, to be conducted annually for 10 years following a patient's surgery.

Specimens from 235 women enrolled in the UNC NBS were selected for the current analysis (Supplementary Figure S1). We analyzed one sample per woman, and included a second specimen for approximately 20% of these women (n = 51, 21.7%) to assess intra-individual variation. Slides were manually reviewed after IHC staining (see below), and 8 samples were excluded due to high levels of non-specific staining. Therefore, the final study population consisted of 228 women and 279 unique tissue samples. Demographic characteristics of our population are presented in Supplementary Table S1.

2.2. Immunohistochemical CD31 staining

Snap-frozen tissue was cut over dry ice and 20-μm sections were cut and mounted on positively charged glass slides. Slides were then randomized to batches of 24 for IHC staining. Briefly, slides were fixed in zinc formalin for 10 minutes, and heat-induced epitope retrieval was performed using Lab Vision HIER Buffer (Thermo Fisher Scientific, Waltham, MA). Slides were then incubated with 3% hydrogen peroxide to block endogenous peroxidases, blocked with 10% normal goat serum for 1 hour at room temperature, and incubated with pre-titrated mouse anti-CD31 antibodies (0.25 μg/mL; #3528, lot #4; Cell Signaling Technologies, Danvers, MA) overnight at 4 °C. Slides were then incubated with biotinylated goat anti-mouse IgG secondary antibodies (#115–065-166, lot #89998; Jackson ImmunoResearch, West Grove, PA) for 1 hour at room temperature, and staining was visualized using ABC Elite (#PK-6100; Vector Laboratories, Burlingame, CA) and diaminobenzidine (DAB; #TA-125-QHDX; Thermo Fisher Scientific) reagents. Antibodies were diluted in Thermo Antibody diluent (#TA-125-ADQ), and all washes were performed with 0.05 M Tris

+0.05% TWEEN-20. Sections were counterstained with hematoxylin.

A negative control (no-primary antibody) slide consisting of human umbilical vein endothelial cells (HUVECs; ATCC, Manassas, VA) grown on chamber slides was included in each batch of stained breast tissue for assessment of secondary antibody non-specific binding. HUVECs maintained in EGM-2 culture medium supplemented with Bullet-Kit reagents (Lonza, Walkersville, MD) were seeded at a density of 50,000 cells/well in 1 well of a 4-well chamber slide (BD Falcon, Franklin Lakes, NJ). Slides were then fixed with 4% paraformaldehyde after 3 days of culture, and stained (1 slide per batch of breast tissue) according to the protocol described above.

2.3. Digital algorithm development and validation

Stained slides were scanned into high-resolution digital images using the Aperio ScanScope XT system (Aperio Technologies, Vista, CA) at a magnification of 20×. Tissue aberrations (eg, large folds, surgical ink) and areas of extensive non-specific staining were excluded via annotation with Aperio ImageScope software. All annotations were made by an investigator blinded to patient demographic information and other tissue characteristics. Annotated images were then imported into Definiens Architect XD version 2.7.0 for analysis with Definiens Tissue Studio version 4.4.2 (Cambridge, MA) (Supplementary Figure S2A). Briefly, a training set consisting of 30 randomly selected slides was constructed, and the tissue and glass components of each specimen were segmented (Supplementary Figure S2B). A Tissue Studio Cellular Analysis Solution capable of detecting and classifying IHC-stained vasculature was then tuned to identify DAB^+ (ie, $CD31^+$) regions. In consideration of previous reports of average capillary diameter [15], and in order to reduce the influence of non-specific staining and other staining artifacts, we set a vascular detection threshold excluding stained objects with cross-sectional areas of $<50\ \mu m^2$. A high-magnification view of the tissue area outlined in Supplementary Figure S2A is shown in Supplementary Figure S2C, and the vascular detection algorithm output of this region is depicted in Supplementary Figure S2D. After the trained algorithm was applied to the entire slide set, digital images were manually reviewed for gross irregularities. Visual inspection suggested high accuracy in identifying vascular areas. However, we identified 75 slides for which the tissue and glass components were not reliably partitioned. Thus, the tissue vs. glass parameter was re-tuned for this subset of slides, leaving all vascular parameters unchanged.

We evaluated the performance of the trained vessel algorithm using a validation set of 33 randomly selected slides. IHC staining levels for each slide were visually classified as low, medium, or high (n = 11 slides/group) by a researcher blinded to patient clinicopathologic characteristics and other tissue features. Automated vessel density measurements for this slide set were then divided into tertiles to evaluate concordance with manual assessment.

2.4. Assessment of breast tissue composition

Epithelial nuclear density, percent adipose, and percent stroma were calculated as metrics of H&E-based tissue composition. These metrics were obtained from the dataset first reported in Sandhu et al [13]. Briefly, to generate this dataset, a validated, previously published Aperio Genie Classifier algorithm [13,14,16,17] was used to partition H&E-stained slides for each NBS participant into regions of adipose, epithelium, and stroma. A validated nuclear detection algorithm included with the Genie Classifier was also used to calculate epithelial nuclear density (nuclei/mm^2 of epithelium). To evaluate associations between tissue composition and vessel density, adipose, epithelial, and stromal content were modeled categorically. For participants with multiple tissue sections, tissue composition values were collapsed prior to categorization by calculating an average estimate weighted by the area of each tissue section. Cubic spline models and boxplots were used to visualize the tissue composition variables to determine appropriate cut-points for categorization. Epithelial nuclear density was classified as <5000, 5000–9000, or >9000 nuclei/mm^2 of epithelium, whereas percent adipose was categorized into quintiles. Percent stroma was modeled as a binary variable dichotomized at 10%: in accordance with findings reported in Chollet-Hinton et al [14], wherein associations between involution (ie, epithelial nuclear density) and breast cancer risk factors were dependent upon stromal context, specimens with ≥10% stromal area were considered "tissue-dense", whereas those with <10% stromal area were considered "tissue non-dense".

2.5. Statistical methods

Multiple linear regression was used to model the associations between vessel density and patient characteristics, tissue composition, and tumor features of unique participants in the NBS. Vessel density was modeled as a log-transformed continuous variable in order to approximate a normal distribution. Patient characteristics included age (categorized by decade), BMI (underweight/normal [<25.0 kg/m^2], overweight [≥25.0 to <30.0 kg/m^2], obese [≥30 kg/m^2]), mammographic density (fatty, scattered fibroglandular, heterogeneously dense, and extremely or not-otherwise-specified dense), and menopausal status (pre-menopausal, post-menopausal). Finally, tumor features included stage (0/1/2, 3/4), grade (1, 2, 3), size (≤2 cm, >2 cm), nodal status (positive, negative), and tumor subtype (hormone receptor [HR]-positive/HER2-negative, HR-negative/HER2-negative, or HER2-positive regardless of HR status). Univariate linear models were used to calculate the crude mean vessel density for each level within explanatory variables. Multivariate analyses (adjusted for either age only or both age and BMI) were used to estimate ratio measures

of the vessel density in each level of the explanatory variables relative to the referent level. Linear tests of trend were conducted assuming a linear dose–response relationship with vessel density for continuous and ordinal variables. Associations for participant and tissue-level characteristics were assessed among all eligible participants (n = 228). Associations for tumor-level characteristics except subtype were assessed among participants with either in situ or invasive breast tumors (n = 209). Associations between vessel density and tumor subtype were assessed only among participants with invasive tumors (n = 180). All statistical analyses were performed using R, version 3.5.1.

3. Results

3.1. Algorithm validation and intra-individual variability in breast tissue vessel density

Data from the vascular density algorithm correlated with manual slide classification and revealed modest intra-individual variability. The vessel density metric exhibited a left-skewed distribution in this study, with nearly half (47.3%) of specimens having <30 vessels/mm^2 of tissue (Fig. 1A), and therefore was modeled on a log scale. The

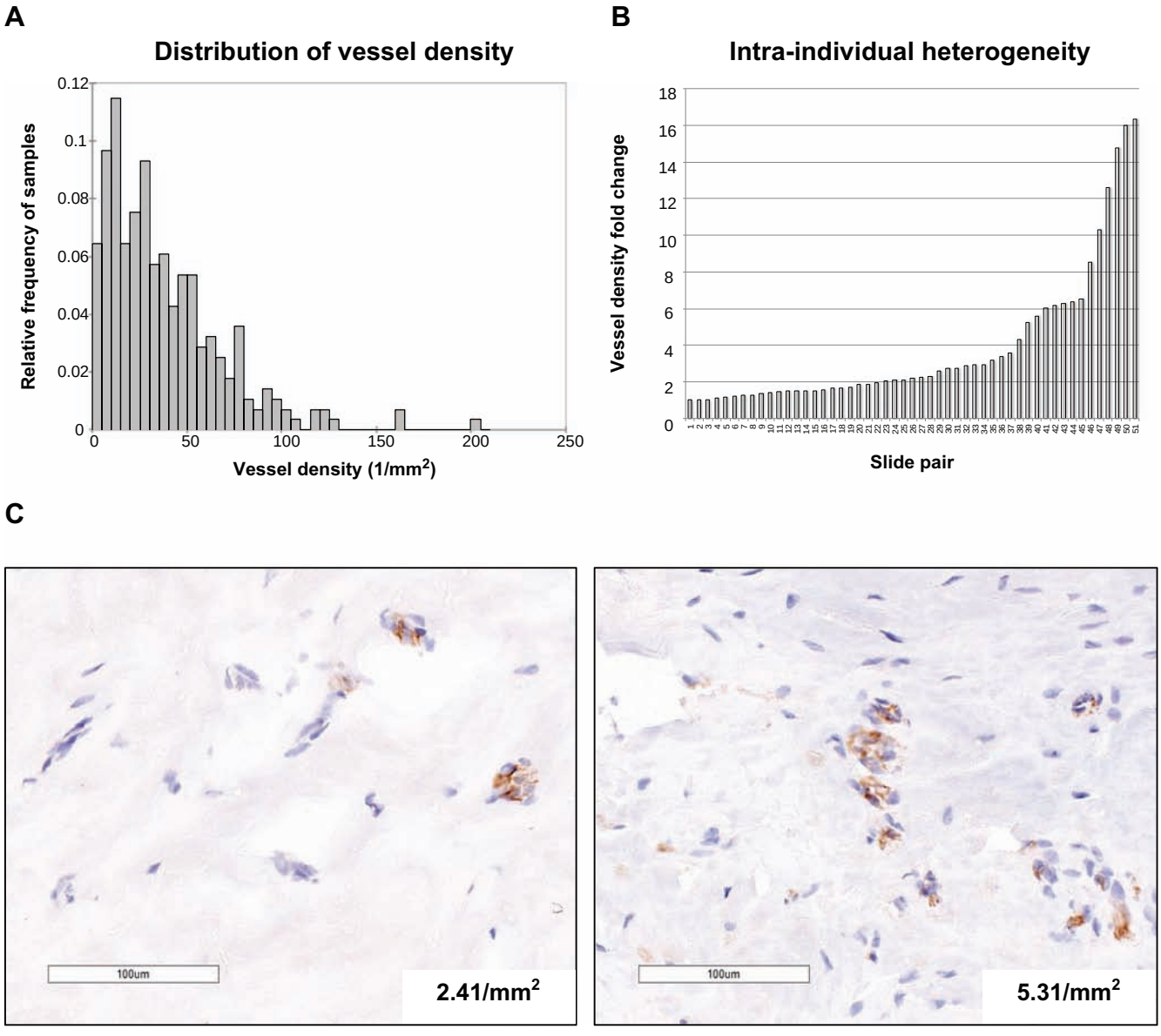

Fig. 1 Distribution and intra-individual heterogeneity of the vessel density metric. A, Histogram depicting the relative frequencies of vessel density values across the study population. B, Vessel density intra-individual heterogeneity of 51 women for whom two slides from different tissue sampling locations were available. For each woman, the vessel density fold-difference between both specimens in a given slide pair is shown. C, Representative images from each specimen in slide pair 26 demonstrating the median observed level of vascular density intra-individual heterogeneity (2.20-fold).

performance of the vascular density algorithm was then assessed with a validation set of 33 slides. Categorical automated and manual slide classification (ie, low, medium, and high vessel density) exhibited 75.8% agreement (Supplementary Figure S3) and "almost perfect" concordance according to accepted benchmarks [18] for interpretation of the Cohen's κ statistic (quadratic-weighted κ: 0.8182; 95% confidence interval [CI]: 0.6946–0.9418). Among 51 women for whom two specimens from different sampling locations were selected, intra-individual heterogeneity in vascular density ranging from 1.00- to 16.3-fold was observed for each sample pair (Fig. 1B). However, for the majority of women, vessel density heterogeneity between the two slides was modest (Fig. 1B). Fig. 1C depicts an example of the median level of observed variation between samples (2.20-fold). Intra-individual heterogeneity (fold-change in vessel density between samples from the same woman) was not associated with tumor characteristics or patient age.

3.2. Associations between vessel density, patient characteristics, and tissue composition

Among patient characteristics, vessel density was most strongly associated with age and BMI (Table 1). Vessel density significantly increased with age (*P*-trend = .0256); therefore, all further analyses were adjusted for decadal age. Vessel density also appeared to increase with increasing

Table 1 Associations between patient characteristics and vessel density from specimens aggregated for unique participants

Patient characteristics	N = 228	Mean (95% CI)	Ratio (95% CI) [a]	*P*-trend [a]	Ratio (95% CI) [b]	*P*-trend [b]
Age						
<40 years	28	17.4 (12.5, 24.2)	0.6 (0.4, 1.0)	.0256	NA	NA
40–49 years	59	27.0 (21.5, 33.8)	REF			
50–59 years	63	33.5 (26.9, 41.7)	1.2 (0.9, 1.7)			
60–69 years	52	29.9 (23.5, 38.0)	1.1 (0.8, 1.5)			
≥70 years	26	34.9 (24.8, 49.1)	1.3 (0.9, 1.9)			
BMI						
Under/normal-weight	75	23.1 (18.8, 28.2)	REF	.0842	NA	NA
Overweight	63	29.7 (23.9, 37.1)	1.2 (0.9, 1.7)			
Obese	90	33.3 (27.7, 40.1)	1.4 (1.1, 1.8)			
Disease status						
Cancer (history or current)	211	28.0 (24.8, 31.6)	REF		REF	
Benign	17	38.1 (24.8, 58.4)	1.5 (0.9, 2.3)	.0952	1.5 (0.9, 2.3)	.0905
Mammographic density [c]						
1 – Fatty	17	24.2 (15.8, 36.9)	0.7 (0.4, 1.1)	.6546	0.7 (0.4, 1.1)	.5034
2 – Scattered fibroglandular	82	33.0 (27.2, 40.0)	REF		REF	
3 – Heterogeneously dense	85	27.9 (23.1, 33.7)	0.9 (0.7, 1.2)		0.9 (0.7, 1.2)	
4 – Dense NOS; extremely dense	24	26.2 (18.4, 37.4)	0.8 (0.6, 1.2)		0.9 (0.6, 1.3)	
Menopausal status						
Pre-menopausal	71	25.2 (20.4, 31.2)	REF	.4408	REF	.2670
Post-menopausal	129	32.0 (27.3, 37.4)	0.8 (0.5, 1.3)		0.8 (0.5, 1.2)	
Tissue characteristics	**N = 228 [d]**	**Mean (95% CI)**	**Ratio (95% CI) [a]**	***P*-trend [a]**	**Ratio (95% CI) [b]**	***P*-trend [b]**
Epithelial nuclear density						
Low (<5000)	97	36.9 (31.2, 43.7)	REF	<.0001	REF	<.0001
Medium (5000–9000)	78	26.5 (21.9, 31.9)	0.7 (0.6, 1.0)		0.7 (0.6, 0.9)	
High (>9000)	49	16.9 (13.4, 21.5)	0.5 (0.4, 0.7)		0.5 (0.4, 0.7)	
Percent adipose						
0–20	36	14.3 (11.0, 18.6)	REF	<.0001	REF	<.0001
20–40	35	24.1 (18.5, 31.4)	1.7 (1.2, 2.4)		1.6 (1.1, 2.4)	
40–60	37	24.1 (18.6, 31.2)	1.6 (1.1, 2.3)		1.6 (1.1, 2.3)	
60–80	57	41.9 (34.1, 51.6)	2.7 (1.9, 3.8)		2.7 (1.9, 3.7)	
80–100	59	37.3 (30.5, 45.8)	2.4 (1.8, 3.4)		2.4 (1.7, 3.4)	
Percent stroma						
<10	79	43.2 (36.0, 51.9)	REF	<.0001	REF	<.0001
≥10	145	21.8 (19.0, 24.9)	0.5 (0.4, 0.6)		0.5 (0.4, 0.7)	

Abbreviation: NA, not available.

[a] Adjusted for decadal age, where appropriate.

[b] Adjusted for decadal age and BMI.

[c] Mammographic density was missing data for 20 participants; *P*-trend was estimated for the ordinal BI-RADS variable.

[d] Epithelial nuclear density, percent adipose, and percent stroma were missing data for 4 participants.

BMI (P-trend = .0842). Although this relationship was only statistically significant among obese women, we conservatively adjusted all further analyses for BMI given reported relationships between obesity and breast cancer (reviewed by Cozzo et al. [19]). Disease status, mammographic density, and menopausal status were not significantly associated with vessel density in univariate or adjusted models.

The associations between vascular density and age or BMI appear to be strongly dependent on tissue composition. The composition of histologically benign human breast tissue varies with age and other breast cancer risk factor exposures [13,14], and even in age-adjusted and age- and BMI-adjusted models, vessel density monotonically decreased with increasing epithelial nuclear density ($P < .0001$; Table 1). Vessel density also exhibited strong positive associations with percent adipose ($P < .0001$; Fig. 2A), and strong inverse associations with percent stroma ($P < .0001$; Fig. 2B). Fig. 2C depicts images of adipose-rich (7.99% of sample) and stroma-rich (82.51% of sample) areas from the same specimen, highlighting that vascular density tends to be much lower in areas of high stromal content.

3.3. Associations between vessel density and tumor characteristics

Given the importance of angiogenesis in tumor progression, we evaluated associations between cancer-adjacent vascular density and tumor clinicopathologic features (Table 2). After adjusting for age, vessel density was significantly reduced in high-stage (stage 3/4; P-trend = .0044), node-negative (P-trend = .0061) tumors, as well as in tumors measuring >2 cm in diameter (P-trend = .0228). These associations were further strengthened in models adjusted for both age and BMI. In contrast, neither tumor grade nor IHC-based tumor subtype exhibited significant associations with vessel density in either adjusted model.

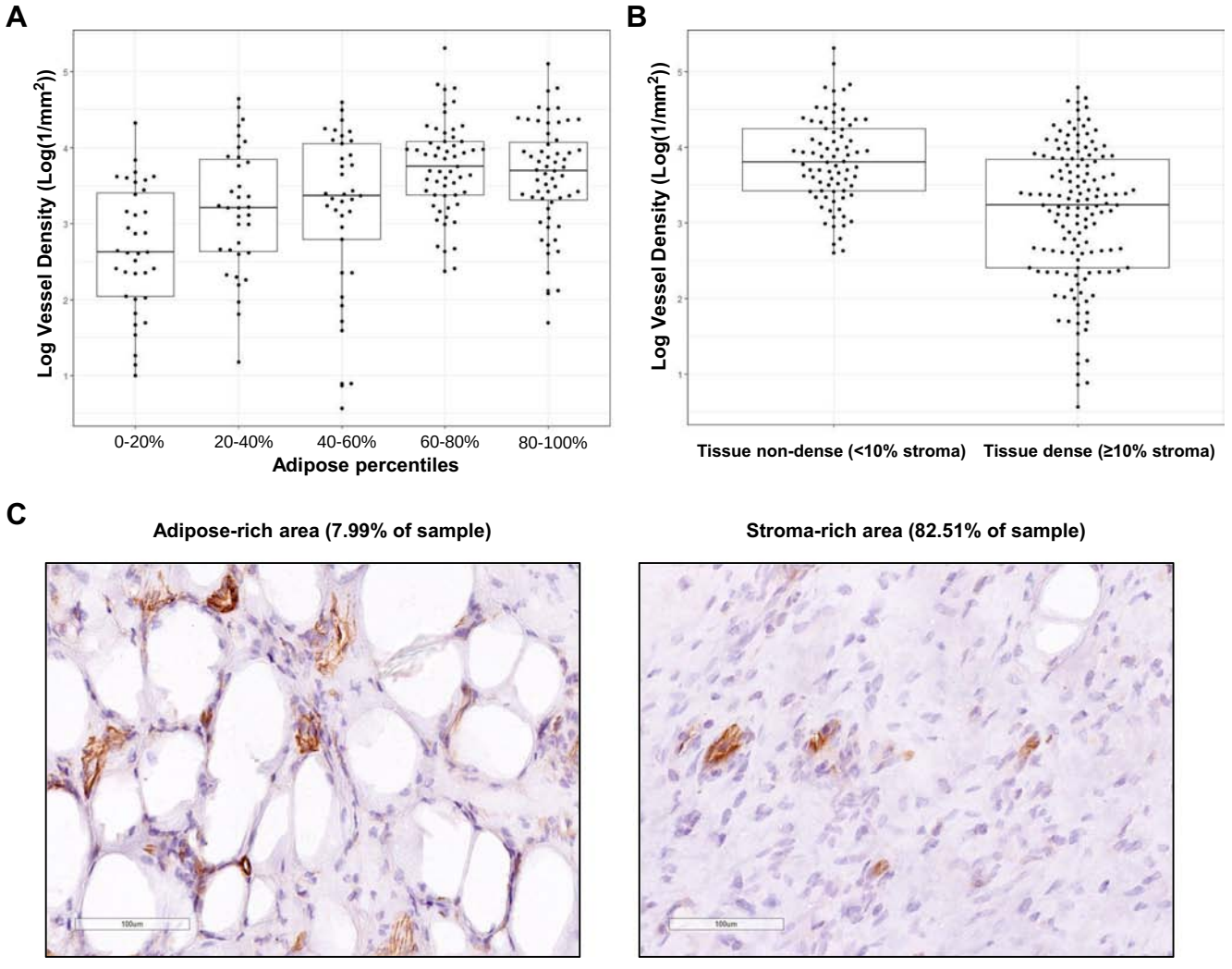

Fig. 2 Associations between vessel density and tissue composition in cancer-adjacent breast. A, Vessel density distribution by adipose quintiles among unique individuals. B, Vessel density distribution by stromal categories among unique individuals. C, Images of an adipose-rich (left) and stroma-rich (right) area from the same specimen, highlighting reductions in vascular density in areas of high stromal content.

Table 2 Associations between tumor characteristics and vessel density among unique specimens from breast cancer patients

Tumor characteristics	N = 209	Mean (95% CI)	Ratio (95% CI) [a]	*P*-trend [a]	Ratio (95% CI) [b]	*P*-trend [b]	Ratio (95% CI) [c]	*P*-trend [c]
Stage								
Early (0/1/2)	177	29.7 (26.1, 33.9)	REF	.0044	REF	.0025	REF	.0556
Late (3/4)	28	18.1 (13.1, 25.1)	0.6 (0.4, 0.9)		0.6 (0.4, 0.8)		0.7 (0.5, 1.0)	
Missing	4							
Grade								
1	40	32.9 (24.9, 43.5)	REF	.7016	REF	.5559	REF	.6049
2	81	26.1 (21.5, 31.8)	0.8 (0.6, 1.1)		0.8 (0.6, 1.1)		0.9 (0.6, 1.2)	
3	85	27.1 (22.4, 32.8)	0.9 (0.7, 1.3)		0.9 (0.6, 1.3)		0.9 (0.7, 1.3)	
Missing	3							
Size								
≤2 cm	112	31.2 (26.4, 36.8)	REF	.0228	REF	.0132	REF	.0592
>2 cm	96	24.4 (20.4, 29.2)	0.8 (0.6, 1.0)		0.7 (0.6, 0.9)		0.8 (0.7, 1.0)	
Missing	1							
Node								
Negative	115	31.7 (27.1, 37.2)	REF	.0061	REF	.0027	REF	.0213
Positive	70	21.1 (17.2, 25.8)	0.7 (0.5, 0.9)		0.7 (0.5, 0.9)		0.8 (0.6, 1.0)	
Missing	24							
Subtype [d]								
HR+HER2-	107	27.4 (23.2, 32.4)	REF	NA	REF	NA	REF	NA
HR-HER2-	30	32.6 (23.8, 44.6)	1.2 (0.9, 1.8)		1.2 (0.9, 1.7)		1.1 (0.8, 1.5)	
HER2+	33	26.8 (19.8, 36.2)	1.1 (0.8, 1.5)		1.1 (0.8, 1.5)		1.2 (0.9, 1.7)	
Missing	10							

Abbreviation: NA, not available.

[a] Adjusted for decadal age.

[b] Adjusted for decadal age and BMI.

[c] Adjusted for decadal age and stromal categories (<10%, ≥10%).

[d] Among invasive tumors (n = 180).

Due to strong associations between vessel density and tissue morphometry metrics, we considered that relationships between tumor features and extratumoral vascularity may also depend on other tissue composition variables. Indeed, after adjusting for stromal content, associations between vascular density, tumor stage, and tumor size reverted toward the null (Table 2). Inverse associations between vascular density and node status were also attenuated, but retained statistical significance (*P*-trend = .0213).

4. Discussion

In this study, we used a digital histologic algorithm to evaluate $CD31^+$ vascular density in histologically benign, cancer-adjacent breast tissue from women with breast cancer. We evaluated 279 specimens from 228 women, increasing the sample size relative to previous studies of normal breast vascular content [11,12] by at least 25–30-fold. Our data indicate that the vascular density of cancer-adjacent breast is related to key demographic variables (eg, age, obesity) and metrics of tissue composition. We further observed that increasing vessel density was associated with positive prognostic tumor features such as lower stage, negative nodal status, and smaller size (<2 cm), although these relationships appear to be largely dependent upon tissue composition.

Prior histologic studies of breast vasculature have predominantly focused on *intratumoral* angiogenesis, showing that high tumor microvessel density is a negative prognostic factor for breast cancer [20]. With respect to extratumoral vasculature, one prior study of high-stage colon cancer cases [21], a murine model of subcutaneously transplanted mammary adenocarcinoma [22], and a rat model of prostate cancer [23] suggested higher extratumoral vessel density or endothelial proliferation in association with increased tumor size. In contrast, findings herein suggest that cancer-adjacent breast vasculature seems to reflect host characteristics rather than tumor biology. However, these studies [21-23] have important differences from the present study of extratumoral benign breast (namely, species and tissue-type), limiting the value of comparison and highlighting the need for further investigation.

In future research evaluating cancer-adjacent breast vascularity, other tissue composition parameters represent important covariates. In the present study, vessel density significantly decreased with increasing epithelial nuclear density and percent stromal area, suggesting that relationships between extratumoral vascularity and cancer behavior may depend upon these other compositional features. Surprisingly, mammographic density and vessel content were not correlated, potentially reflecting the nature of mammographic density as a composite metric of fibroglandular (epithelial and stromal) breast tissue content. Relationships between cancer phenotypes and

extratumoral vascularity may also depend upon breast adipose tissue content, as vascular density significantly increased with both obesity (BMI $\geq$30 kg/m^2) and percent breast adiposity. Interestingly, work by Condeelis and colleagues has demonstrated that an increased frequency of tumor microenvironments of metastasis (TMEMs), or histologic structures in which a Mena-overexpressing cancer cell, an endothelial cell, and a macrophage are in direct contact, predicts risk of distant metastasis among ER$^+$ breast cancer patients independently of classical tumor clinicopathologic features [24,25]. Thus, together with these observations, reports that obese and older women experience higher frequencies of ER$^+$ tumors (reviewed by Picon-Ruiz et al. [26]), and previous findings that macrophage content is increased in normal breast tissue from obese compared to normal-weight women [27], our results provide biological plausibility for previously described associations [8-10] between obesity and reduced survivorship among ER$^+$ breast cancer patients.

Few previous studies have evaluated vascular density in association with age, though, to our knowledge, none have focused on breast tissue. Gunin et al reported that the density of CD31$^+$ dermal blood vessels significantly declined with age [28], and an in vivo imaging study by Li and colleagues revealed that the density of capillary loops in the superficial vascular plexus of the hand negatively correlated with age [29]. Reduced tissue perfusion and associated visceral functional deficits have also been attributed to impaired angiogenesis in models of the aging kidney [30], liver [31], and retina [32]. Differences between these reports and the present study may be due to tissue site-specificity, as well as with age-associated differences in breast tissue composition [13]. These findings further underscore the complex dynamic interplay between various tissue components.

Our study should be interpreted in light of certain limitations. First, although CD31 is generally considered to be the single best indicator of endothelial differentiation status [33], this marker can also be expressed on hematopoietic lineage cells such as neutrophils and macrophages [34]. However, based upon extensive visual inspection of our slide set, we anticipate that this phenomenon exerts little impact on our results. Second, the H&E-based tissue morphometry dataset leveraged herein was generated from separate sections from the same tissue block as the CD31-stained sections. Thus, some variation may exist in the proportions of stroma, adipose, and epithelium between the corresponding CD31- and H&E-stained slides. However, a previous study of tissue morphometry in the NBS indicated that estimates of each tissue component were highly correlated between replicate measurements in a given patient [13]. Furthermore, our results may be influenced by the high prevalence of overweight and obesity among women in our sample (BMI $\geq$25.0 kg/m^2; 67.1% of women), highlighting the need to evaluate vascular density in a greater number of breast samples from normal-weight women. Finally, our work could be strengthened by the inclusion of a greater number of specimens from women with no invasive breast cancer history. However, with the exception of reduction mammoplasty (RM) samples, which display a high prevalence of benign disease and/or proliferative change relative to non-RM tissue [35], specimens of this nature are not readily available. Nevertheless, in spite of these limitations, few previous studies of normal human breast vasculature have been reported, and those that have relied on tissue from a small or unspecified number of women with relatively homogeneous demographic characteristics [11,12]. Thus, the present study is an important first step in understanding how tumor-adjacent vasculature varies in association with tumor characteristics and associated breast cancer risk factors in more heterogeneous samples.

In conclusion, this study highlighted the importance of breast composition in determining extratumoral vascularity, and highlighted an inverse association between extratumoral vascular density and aggressive tumor characteristics. We were not able to evaluate the association between vascularity and adiposity within strata of tumor subtypes; however, adiposity is associated with reduced survivorship among ER$^+$ breast cancer patients [8-10], and higher vascular content in histologically benign tissue from obese women may be a plausible biological explanation for these observations. Continued research to understand the vascular features of normal-appearing, cancer-adjacent tissue may have important implications for assessing patterns of disease metastasis and recurrence among cancer patients.

Supplementary data

Supplementary data to this article can be found online at https://doi.org/10.1016/j.humpath.2019.06.003.

References

[1] Folkman J, Long Jr DM, Becker FF. Growth and metastasis of tumor in organ culture. Cancer 1963;16:453-67.
[2] Siemann DW. The unique characteristics of tumor vasculature and preclinical evidence for its selective disruption by tumor-vascular disrupting agents. Cancer Treat Rev 2011;37(1):63-74.
[3] Casbas-Hernandez P, et al. Tumor intrinsic subtype is reflected in cancer-adjacent tissue. Cancer Epidemiol Biomarkers Prev 2015;24 (2):406-14.
[4] Graham K, et al. Gene expression profiles of estrogen receptor-positive and estrogen receptor-negative breast cancers are detectable in histologically normal breast epithelium. Clin Cancer Res 2011;17(2): 236-46.
[5] Finak G, et al. Stromal gene expression predicts clinical outcome in breast cancer. Nat Med 2008;14(5):518-27.
[6] Roman-Perez E, et al. Gene expression in extratumoral microenvironment predicts clinical outcome in breast cancer patients. Breast Cancer Res 2012;14(2):R51.
[7] Troester MA, et al. DNA defects, epigenetics, and gene expression in cancer-adjacent breast: a study from the Cancer Genome Atlas. NPJ Breast Cancer 2016;2:16007.
[8] Sparano JA, et al. Obesity at diagnosis is associated with inferior outcomes in hormone receptor-positive operable breast cancer. Cancer 2012;118(23):5937-46.

[9] Fontanella C, et al. Impact of body mass index on neoadjuvant treatment outcome: a pooled analysis of eight prospective neoadjuvant breast cancer trials. Breast Cancer Res Treat 2015;150(1):127-39.
[10] Cecchini RS, et al. Body mass index at diagnosis and breast Cancer survival prognosis in clinical trial populations from NRG oncology/NSABP B-30, B-31, B-34, and B-38. Cancer Epidemiol Biomarkers Prev 2016;25(1):51-9.
[11] Naccarato AG, et al. Definition of the microvascular pattern of the normal human adult mammary gland. J Anat 2003;203(6):599-603.
[12] Sigurdsson V, et al. Human breast microvascular endothelial cells retain phenotypic traits in long-term finite life span culture. In Vitro Cell Dev Biol Anim 2006;42(10):332-40.
[13] Sandhu R, et al. Digital histologic analysis reveals morphometric patterns of age-related involution in breast epithelium and stroma. Hum Pathol 2016;48:60-8.
[14] Chollet-Hinton L, et al. Stroma modifies relationships between risk factor exposure and age-related epithelial involution in benign breast. Mod Pathol 2018;1:211.
[15] Freitas RA. *Nanomedicine, Volume 1: Basic Capabilities*. Vol. 1. Austin, TX: Landes Bioscience; 1999.
[16] Sun X, et al. Relationship of mammographic density and gene expression: analysis of normal breast tissue surrounding breast cancer. Clin Cancer Res 2013;19(18):4972-82.
[17] Sun X, et al. Benign breast tissue composition in breast cancer patients: association with risk factors, clinical variables, and gene expression. Cancer Epidemiol Biomarkers Prev 2014;23(12):2810-8.
[18] Landis JR, Koch GG. The measurement of observer agreement for categorical data. Biometrics 1977;33(1):159-74.
[19] Cozzo AJ, Fuller AM, Makowski L. Contribution of adipose tissue to development of Cancer. Compr Physiol 2017;8(1):237-82.
[20] Uzzan B, et al. Microvessel density as a prognostic factor in women with breast cancer: a systematic review of the literature and meta-analysis. Cancer Res 2004;64(9):2941-55.
[21] Fox SH, et al. Angiogenesis in normal tissue adjacent to colon cancer. J Surg Oncol 1998;69(4):230-4.
[22] Thompson WD, et al. Tumours acquire their vasculature by vessel incorporation, not vessel ingrowth. J Pathol 1987;151(4):323-32.
[23] Halin S, et al. Extratumoral macrophages promote tumor and vascular growth in an orthotopic rat prostate tumor model. Neoplasia 2009;11(2):177-86.
[24] Robinson BD, et al. Tumor microenvironment of metastasis in human breast carcinoma: a potential prognostic marker linked to hematogenous dissemination. Clin Cancer Res 2009;15(7):2433-41.
[25] Rohan TE, et al. Tumor microenvironment of metastasis and risk of distant metastasis of breast cancer. J Natl Cancer Inst 2014;106(8).
[26] Picon-Ruiz M, et al. Obesity and adverse breast cancer risk and outcome: mechanistic insights and strategies for intervention. CA Cancer J Clin 2017;67(5):378-97.
[27] Sun X, et al. Normal breast tissue of obese women is enriched for macrophage markers and macrophage-associated gene expression. Breast Cancer Res Treat 2012;131(3):1003-12.
[28] Gunin AG, et al. Age-related changes in angiogenesis in human dermis. Exp Gerontol 2014;55:143-51.
[29] Li L, et al. Age-related changes of the cutaneous microcirculation in vivo. Gerontology 2006;52(3):142-53.
[30] Kang DH, et al. Impaired angiogenesis in the aging kidney: vascular endothelial growth factor and thrombospondin-1 in renal disease. Am J Kidney Dis 2001;37(3):601-11.
[31] Ito Y, et al. Age-related changes in the hepatic microcirculation in mice. Exp Gerontol 2007;42(8):789-97.
[32] Grunwald JE, et al. Effect of aging on retinal macular microcirculation: a blue field simulation study. Invest Ophthalmol Vis Sci 1993;34(13):3609-13.
[33] Pusztaszeri MP, Seelentag W, Bosman FT. Immunohistochemical expression of endothelial markers CD31, CD34, von Willebrand factor, and Fli-1 in normal human tissues. J Histochem Cytochem 2006;54(4):385-95.
[34] Ross EA, et al. CD31 is required on CD4+ T cells to promote T cell survival during *Salmonella* infection. J Immunol 2011;187(4):1553-65.
[35] Sherman ME, et al. The Susan G. Komen for the Cure tissue Bank at the IU Simon Cancer center: a unique resource for defining the "molecular histology" of the breast. Cancer Prev Res (Phila) 2012;5(4):528-35.